Electronic Supplementary Material (ESI) for Lab on a Chip.


# Electronic supplementary information

## OSTE+ for in-situ SAXS Analysis with Droplet Microfluidic Devices

Tobias Lange,[a,b] Sophie Charton,[b] Thomas Bizien,[c] Fabienne Testard[a] and Florent Malloggi[a,*]

[a] Université Paris-Saclay, CEA, CNRS, NIMBE, CEA Saclay, 91191 Gif-sur-Yvette Cedex, France.
[b] CEA, DES, ISEC, DMRC, Univ. Montpellier, Marcoule, France.
[c] Synchrotron SOLEIL, l'Orme des Merisiers, Saint-Aubin - BP 48, 91192 Gif-sur-Yvette Cedex, France.

July 7, 2020

## Contents

# 1 Gold Nanoparticles

Gold nanoparticles were produced from a reverse Turkevich method following the protocol described by Sivaraman et al.[1] 250 µL of aqueous 25.4 mM $HAuCl_4$ solution was added rapidly to 24.75 mL of 5.2 mM boiling citrate solution under vigorous stirring. Boiling was stopped after 250 s and the solution was let without stirring for 12 h before being used. The nanoparticles were characterized by SAXS and Transmission electron microscopy (TEM) and have a diameter of 9.4 nm $\pm$ 1.0 nm.

TEM was performed on a Philips CM12 electron microscope operated at 80 kV. A drop of the solution was deposited on a copper grid covered with a carbon film (Agar Scientific). The excess liquid was blotted off with filter paper after a few seconds.

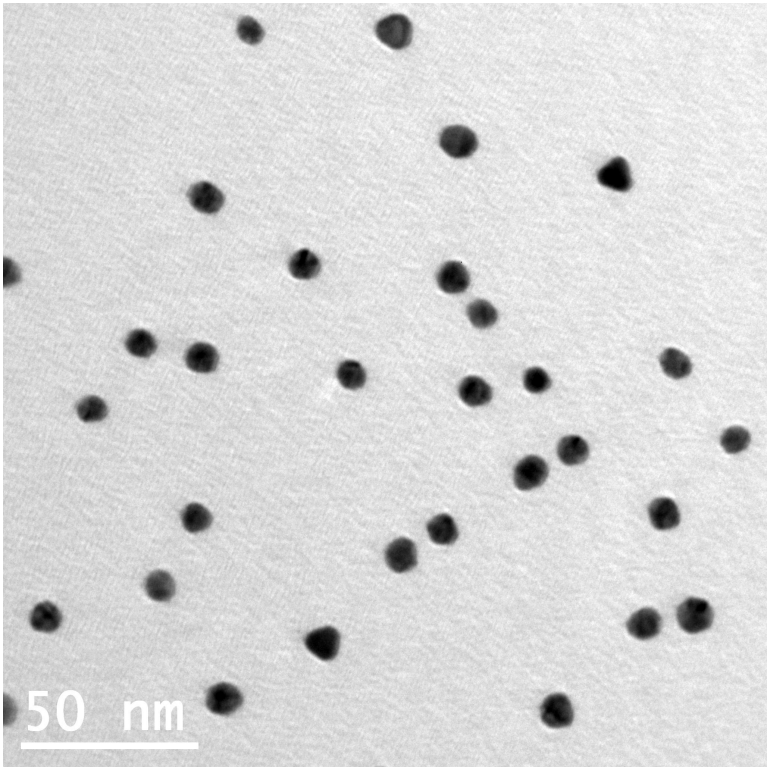


Figure S1: TEM micrograph of the synthesized gold nanoparticles.

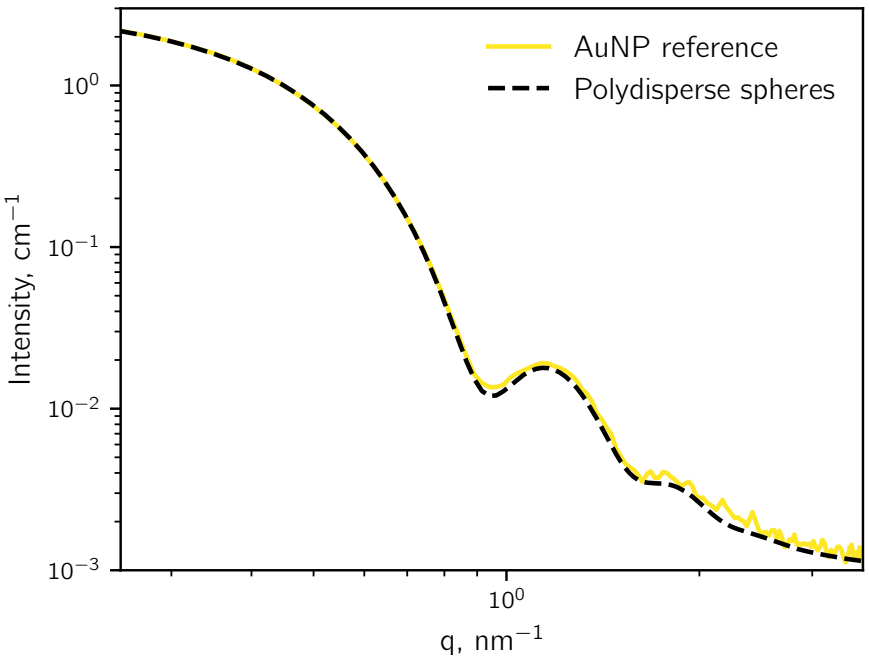


Figure S2: SAXS pattern of the synthesized gold nanoparticles and a fit by polydisperse spheres. The fit yields a mean diameter of 9.4 nm $\pm$ 1.0 nm and a particle concentration of $8.8 \times 10^{12}\,\mathrm{cm}^{-3}$. The scattering length density (SLD) of the particles is $1.314 \times 10^{12}\,\mathrm{cm}^{-3}$ and the SLD of the medium is $9.396 \times 10^{10}\,\mathrm{cm}^{-3}$. A background of $1 \times 10^{-3}\,\mathrm{cm}^{-1}$ is added.

# 2 Master preparation

Si/WBR masters were prepared by laminating layers of dryfilm (50 µm thick WBR2050 and 100 µm thick WBR2100, Dupont) with a hot roll laminator (ZX-J series HF-380, Innovo) onto a Si wafer (diameter 10 cm, Sil'Tronix Silicon Technologies). After the lamination, microstructures were created by photolithography. To create a photomask the device structure was designed with the help of a computer-aided design program and printed on a flexible polyester film by a commercial service (JD Photo Data, UK).

Before laminating the wafer it was degreased with acetone (99 %, Honeywell) and blow-dried with pressurized air. The first film layer was roughly cut to size and the protective polyethylene layer was removed by using sticky tape, before placing the wafer on a supporting metal plate (Cu, 1 mm thick). Then, the dryfilm was aligned to it with the unprotected side facing the wafer. To reduce wrinkling of the film, the dryfilm was brought into contact with the metal support on the advancing side of the wafer before starting the roll laminator and the film was kept under tension during the lamination (Figure S3). The lamination temperature was 85 °C and the lamination speed was approximately 24 mm $s^{-1}$. After lamination, the wafer was turned upside down and the excess dryfilm was removed. To apply a second layer of dryfilm, the protective polyester layer on top of the wafer-WBR stack was removed by using sticky tape and the procedure was repeated. The adhesion between the film and the substrate was improved by baking the piece over night at 60 °C in an oven. After the item reached room temperature, the protective polyester layer was removed by using sticky tape, a photomask was aligned and brought into contact with the film. The assembly was then exposed to UV light for 20 s at 48.8 mW $cm^{-1}$ (365 nm, UV-Kub 2, Kloé). Before development, the excess of dryfilm was removed with a razor blade and it was baked at 100 °C for 60 s on a hot plate (C-MAG HP 10, IKA). After cooling down, it was developed by applying a stream of 1 % $K_2CO_3$ solution with a peristaltic pump (101U, Watson Marlow) until no undeveloped film was visible anymore. To finish the development it was washed with tap water and carefully blow dried with pressurized air.

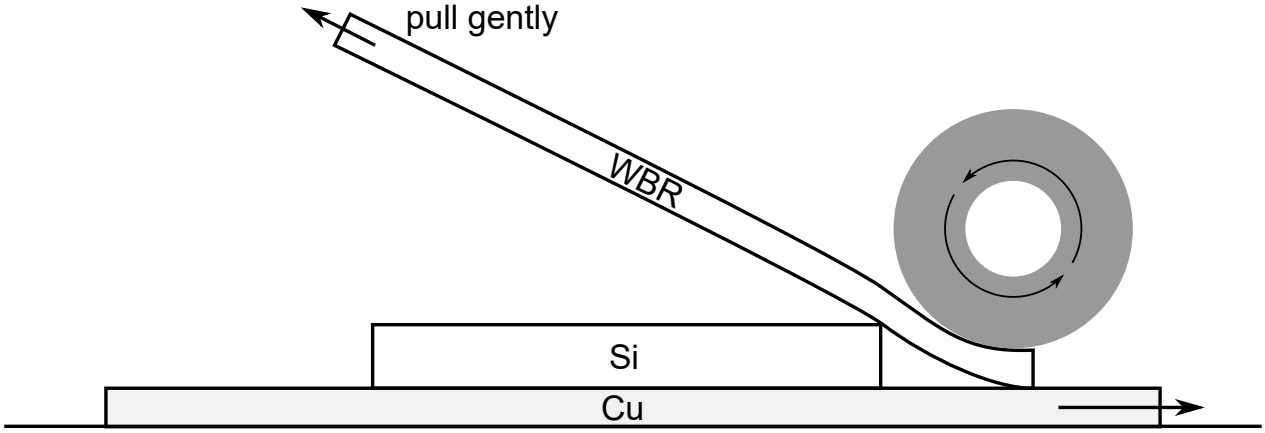


Figure S3: Lamination of WBR dryfilm onto a Si wafer with a hot-roll laminator. By gently pulling the dryfilm during lamination, it is kept under tension and the final laminate is wrinkle free.

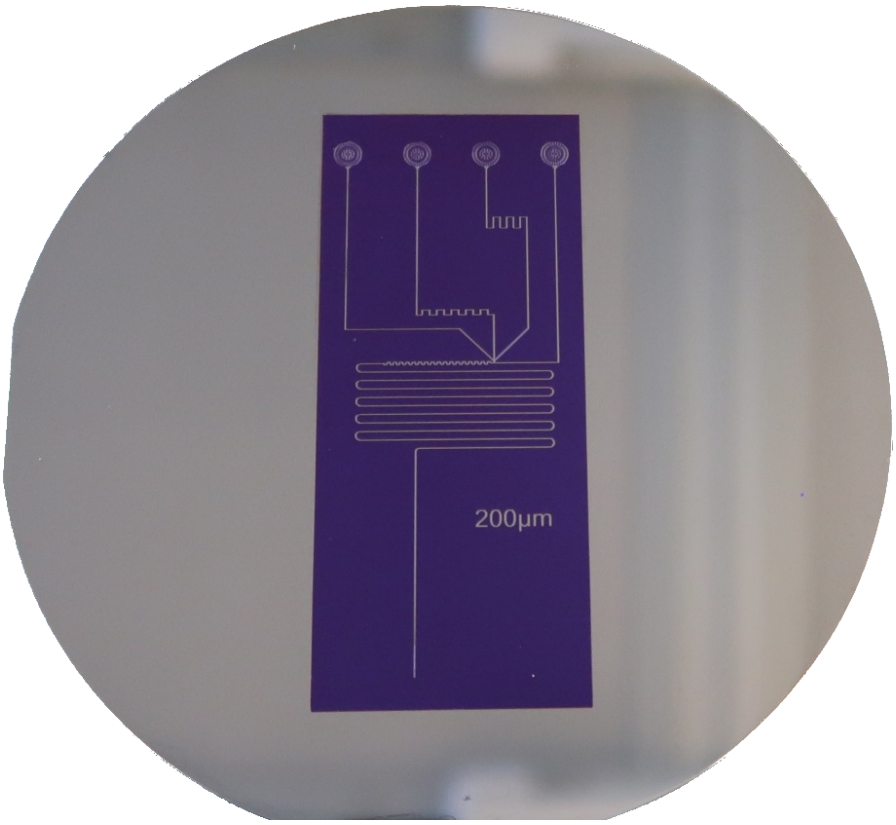


Figure S4: Finished Si/WBR master.

# 3 Tube-chip-interface

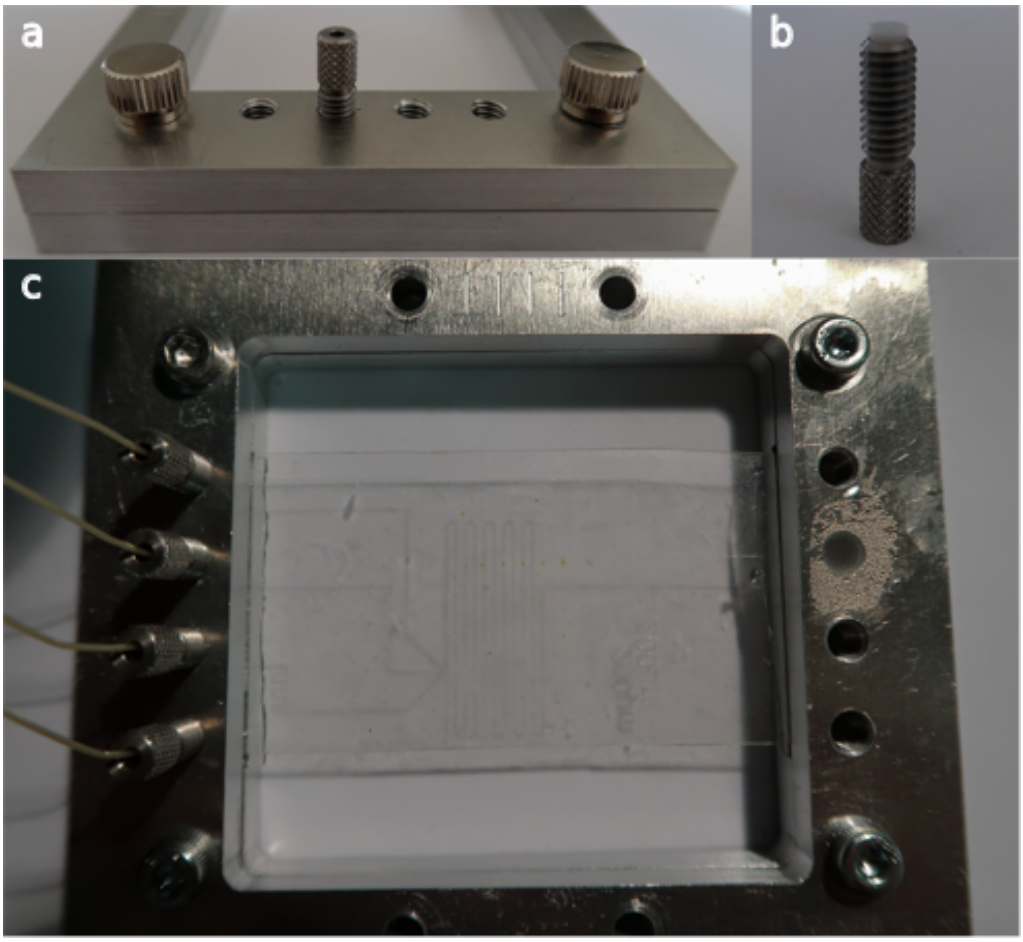


Figure S5: **a:** IMT device holder with tube connector. **b:** IMT tube connector with PTFE gasket. **c:** Mounted Chip with connected inlets.

# 4 Experimental Set-up

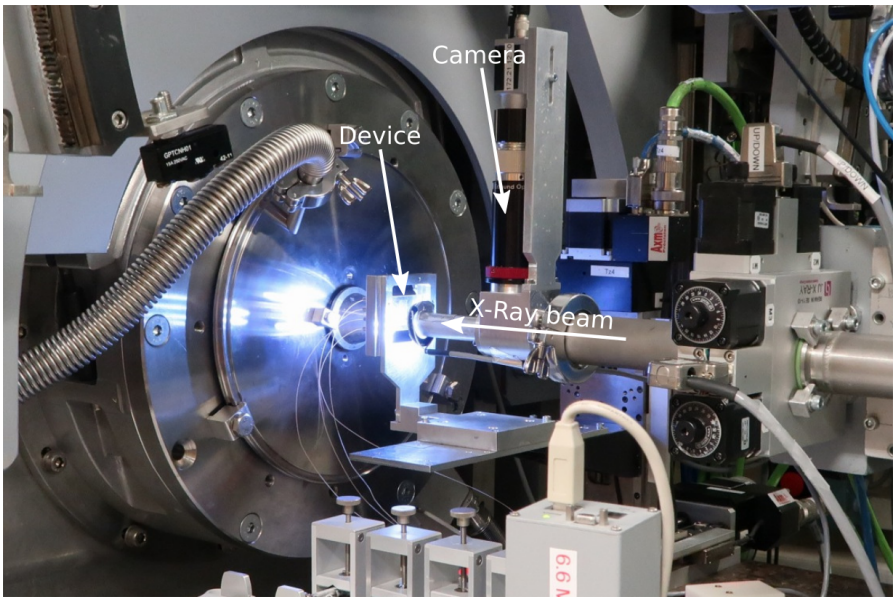


Figure S6: Experimental set-up at the SWING beam line.

# 5 Thermal Aging

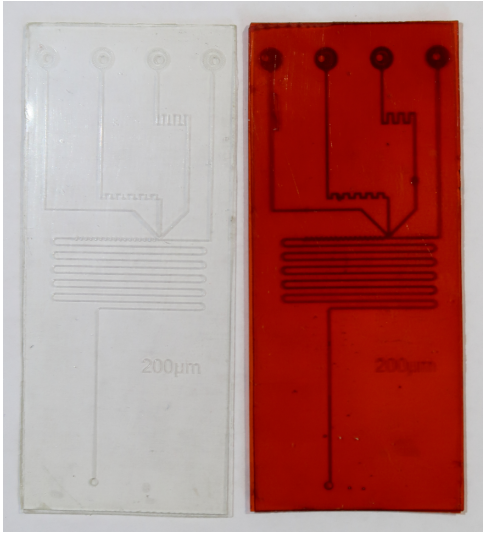


Figure S7: **Left:** OSTE+ device after normal curing at 90 °C. **Right:** OSTE+ device after additional curing at 150 °C for 7 days.

# 6 Staining

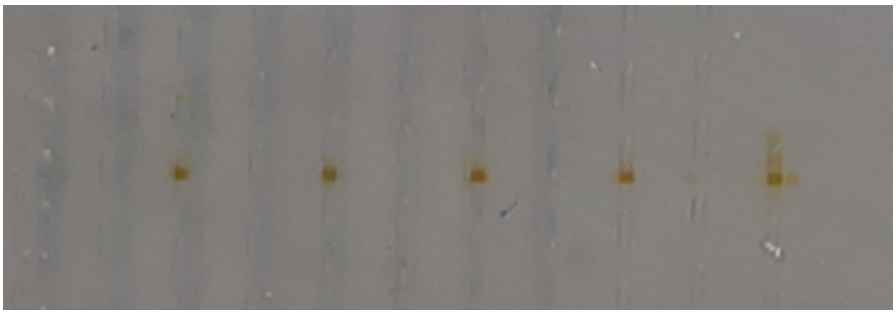

Figure S8: Staining observed on an OSTE+ device after an in-situ experiment.

# 7 Extraction

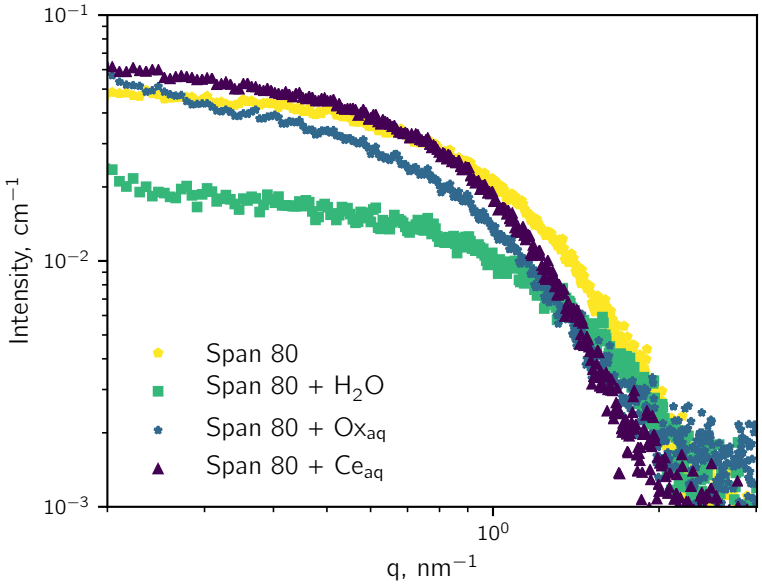


Figure S9: SAXS patterns of 1 % Span 80 (w/w) in light mineral oil before and after equilibration with $H_2O$, 0.15 M $H_2C_2O_4$ ($Ox_{aq}$) and 0.10 M $Ce(NO_3)_3$ ($Ce_{aq}$). Background and scattering of light mineral oil are subtracted. Data collected at 8.04 keV (XEUSS 2.0).

Before equilibration, the scattering of small spherical objects is visible. After equilibration with water, the scattering intensity decreases. The reverse micelles swell by water and the scattering length density of the micelle core decreases Due to the corresponding decrease in electronic contrast between the micelle core and the alkyl chain of the surfactant, the observed scattering intensity decreases as well. No decrease is observable for the solutions that contain reactants, an increase which might indicate a higher scattering length density in the reverse micelle core caused by the presence of oxalic acid or cerium nitrate. In addition, the scattering signal intensity around 1 nm decreases at a lower q value, which indicates a larger particle size for the reverse micelles that contain $Ce(NO_3)_3$ or oxalic acid, compared to water alone. Fitting the equilibrated scattering patterns with a model of polydisperse spheres yields an approximate size of 3.6 nm $\pm$ 0.8 nm for the Span 80 alone, 4.4 nm $\pm$ 0.6 nm for equilibration with 0.10 M oxalic acid and 4.6 nm $\pm$ 0.6 nm for equilibration with 0.15 M $Ce(NO_3)_3$.

# 8 Droplet Scattering

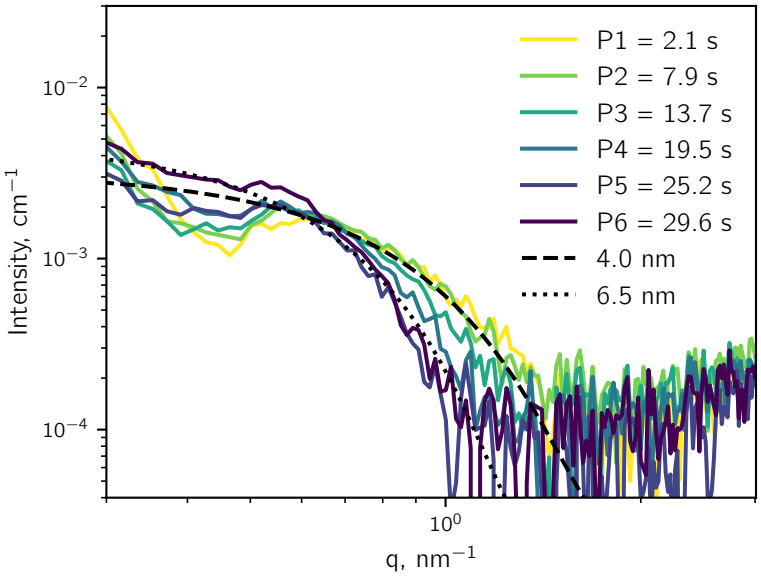


Figure S10: Droplet scattering patterns after subtraction of the $q^{-3}$ slope. The broken lines indicate the scattering signal that would be generated by spherical objects of $4.0 \pm 1.0$ and $6.5 \pm 1.0$ nm diameter.

# 9 Stopped droplet

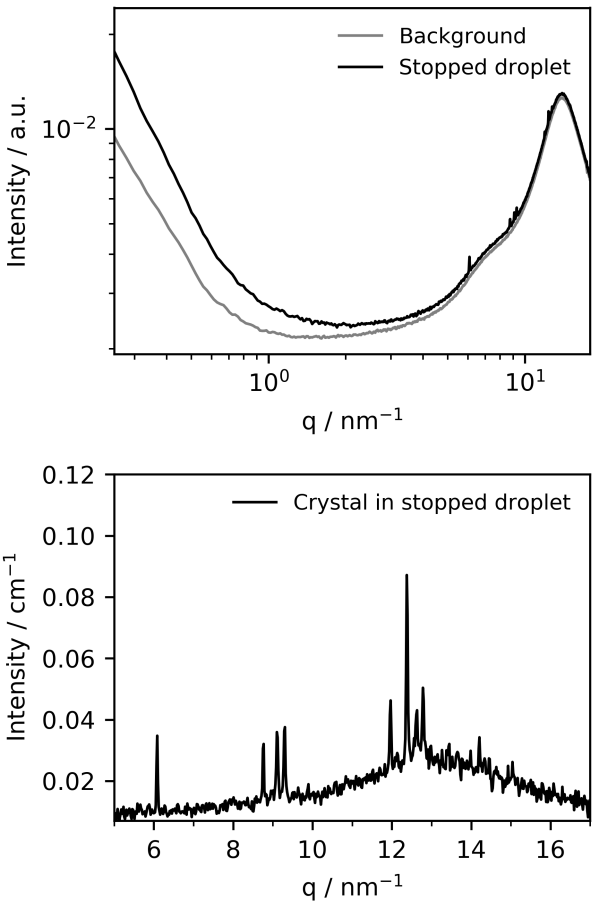


Figure S11: **Top:** SAXS patterns of binary solvent and a droplet with growing crystals inside. **Bottom:**. Typical Bragg peaks of cerium oxalate are visible after the data treatment.

# References

[1] S. K. Sivaraman, S. Kumar and V. Santhanam, *Journal of colloid and interface science*, 2011, **361**, 543–547.